

Chronic Active Lesions and Larger Choroid Plexus Explain Cognition and Fatigue in Multiple Sclerosis

Paolo Preziosa, MD, PhD, Elisabetta Pagani, MSc, Alessandro Meani, MSc, Loredana Storelli, PhD, Monica Margoni, MD, PhD, Yury Yudin, MD, Nicolò Tedone, MSc, Diana Biondi, MSc, Martina Rubin, MD, Maria A. Rocca, MD, and Massimo Filippi, MD

Correspondence
Prof. Filippi
filippi.massimo@hsr.it

Neurol Neuroimmunol Neuroinflamm 2024;11:e200205. doi:10.1212/NXI.000000000200205

Abstract

Background and Objectives

Chronic inflammation may contribute to cognitive dysfunction and fatigue in patients with multiple sclerosis (MS). Paramagnetic rim lesions (PRLs) and choroid plexus (CP) enlargement have been proposed as markers of chronic inflammation in MS being associated with a more severe disease course. However, their relation with cognitive impairment and fatigue has not been fully explored yet. Here, we investigated the contribution of PRL number and volume and CP enlargement to cognitive impairment and fatigue in patients with MS.

Methods

Brain 3T MRI, neurologic evaluation, and neuropsychological assessment, including the Brief Repeatable Battery of Neuropsychological Tests and Modified Fatigue Impact Scale, were obtained from 129 patients with MS and 73 age-matched and sex-matched healthy controls (HC). PRLs were identified on phase images of susceptibility-weighted imaging, whereas CP volume was quantified using a fully automatic method on brain three-dimensional T1-weighted and fluid-attenuated inversion recovery MRI sequences. Predictors of cognitive impairment and fatigue were identified using random forest.

Results

Thirty-six (27.9%) patients with MS were cognitively impaired, and 31/113 (27.4%) patients had fatigue. Fifty-nine (45.7%) patients with MS had ≥ 1 PRLs (median = 0, interquartile range = 0;2). Compared with HC, patients with MS showed significantly higher T2-hyperintense white matter lesion (WM) volume; lower normalized brain, thalamic, hippocampal, caudate, cortical, and WM volumes; and higher normalized CP volume (p from <0.001 to 0.040). The predictors of cognitive impairment (relative importance) (out-of-bag area under the curve [OOB-AUC] = 0.707) were normalized brain volume (100%), normalized caudate volume (89.1%), normalized CP volume (80.3%), normalized cortical volume (70.3%), number (67.3%) and volume (66.7%) of PRLs, and T2-hyperintense WM lesion volume (64.0%). Normalized CP volume was the only predictor of the presence of fatigue (OOB-AUC = 0.563).

Discussion

Chronic inflammation, with higher number and volume of PRLs and enlarged CP, may contribute to cognitive impairment in MS in addition to gray matter atrophy. The contribution of enlarged CP in explaining fatigue supports the relevance of immune-related processes in determining this manifestation independently of disease severity. PRLs and CP enlargement may contribute to the pathophysiology of cognitive impairment and fatigue in MS, and they may represent clinically relevant therapeutic targets to limit the impact of these clinical manifestations in MS.

From the Neuroimaging Research Unit (P.P., E.P., A.M., L.S., M.M., Y.Y., N.T., D.B., M.R., M.A.R., M.F.), Division of Neuroscience; Neurology Unit (P.P., M.M., M.R., M.A.R., M.F.), IRCCS San Raffaele Scientific Institute; Vita-Salute San Raffaele University (P.P., M.R., M.A.R., M.F.); Neurorehabilitation Unit (M.M., M.F.); and Neurophysiology Service (M.F.), IRCCS San Raffaele Scientific Institute, Milan, Italy.

Go to [Neurology.org/NN](https://www.neurology.org/NN) for full disclosures. Funding information is provided at the end of the article.

The Article Processing Charge was funded by the authors.

This is an open access article distributed under the terms of the Creative Commons Attribution-NonCommercial-NoDerivatives License 4.0 (CC BY-NC-ND), which permits downloading and sharing the work provided it is properly cited. The work cannot be changed in any way or used commercially without permission from the journal.

Glossary

BRB-N = Brief Repeatable Battery of Neuropsychological Tests; **CP** = choroid plexus; **EDSS** = Expanded Disability Status Scale; **ETL** = echo train length; **FDR** = false discovery rate; **FLAIR** = fluid-attenuated inversion recovery; **FOV** = field of view; **GM** = gray matter; **HC** = healthy control; **IQR** = interquartile range; **MFIS** = Modified form of the Fatigue Impact Scale; **MS** = multiple sclerosis; **OOB-AUC** = out-of-bag area under the curve; **PASAT** = Paced Auditory Serial Addition Test; **PRLs** = paramagnetic rim lesions; **SDMT** = Symbol Digit Modalities Test; **SWI** = susceptibility-weighted imaging; **TE** = echo time; **TI** = inversion time; **TR** = repetition time; **WM** = white matter lesion.

Introduction

Cognitive impairment and fatigue have been reported in up to 70% and 80% of patients with multiple sclerosis (MS), occur from the earliest phases of the disease, and have a detrimental impact on patients' daily life activities and quality of life.^{1,2}

Recent MRI studies have consistently shown that complex mechanisms may explain cognitive dysfunction in MS.^{1,3,4} These include a "disconnection syndrome" caused by the accumulation of focal lesions and microstructural tissue abnormalities in cognitively related white matter (WM) tracts, the occurrence of focal and diffuse damage in strategic gray matter (GM) regions, and the presence of functional brain network abnormalities reflecting a progressive failure of the adaptive capacity of the brain.³⁻⁵ On the other hand, fatigue has been associated with abnormal functional activity in several brain regions mainly involving frontoparietal cortices and the basal ganglia,^{6,7} together with the presence of focal WM lesions, microstructural WM abnormalities, and GM atrophy of regions including prefrontal cortices, thalamus, and caudate nucleus.^{6,7}

Recent pathologic and MRI studies have supported the role of chronic inflammation as one of the most relevant drivers of a more severe disability progression in MS.⁸ In particular, chronic active lesions and choroid plexus (CP) enlargement have been suggested as 2 clinically relevant proxies of chronic inflammation that can be explored *in vivo* using MRI.

Chronic active lesions are pathologically typified by a peripheral "rim" of iron-laden activated microglia/macrophages associated with ongoing demyelination and axonal loss around an inactive core without blood-brain barrier damage.^{9,10} These lesions show a paramagnetic hypointense rim (i.e., paramagnetic rim lesions [PRLs]) on susceptibility-based MRI sequences that corresponds to the peripheral activated iron-laden microglia.^{9,10} In MS, PRLs have been associated with more severe clinical disability, progressive disease course, and brain atrophy.^{10,11}

The CP plays a key role in the immunologic regulation within the CNS since it acts as an interface between the peripheral immune system and CNS.¹² A significant enlargement of the CP occurs from the earliest phases of MS and is associated with higher relapse rate, higher brain T2-hyperintense WM

lesion volume and inflammatory activity, and more severe disability progression.¹³⁻¹⁷

A higher PRL burden and CP enlargement, reflecting a chronic proinflammatory environment, are likely to contribute to both worse cognitive performance and fatigue, possibly through the promotion of progressive demyelination, neuro-axonal damage, and synaptic loss.¹⁸ However, at present, the relation of chronic inflammation with cognitive impairment has been only partially explored,^{10,19,20} whereas no study investigated its association with fatigue. Patients with MS with at least 1^{19,20} or 4 PRLs¹⁰ showed worse cognitive performance and reached cognitive impairment at a younger age. A significantly higher CP volume was also found to be associated with worse cognitive performance.²¹ However, these studies did not include a comprehensive neuropsychological battery, but only include some neuropsychological tests, such as the Paced Auditory Serial Addition Test (PASAT), the Symbol Digit Modalities Test (SDMT), or the California Verbal Learning Test-II.^{10,19,20} Moreover, patients with MS were grouped according to the presence or not of at least 1 or 4 PRLs, the volume of PRLs was not evaluated, and it remained unclear whether the association with cognitive impairment was specific for PRLs.

By evaluating a large and well-characterized cohort of patients with MS including the main disease clinical phenotypes, here we evaluated the prevalence and volume of PRLs as well as the presence CP enlargement in patients with MS. Then, we investigated whether, in addition to volumetric measures of brain WM lesions and of strategic GM regions involved in cognitive functions and fatigue (i.e., thalamus caudate nucleus, hippocampus, and brain cortex), PRL number and volume and CP volume were also included among the significant MRI predictors of cognitive impairment and fatigue.

Methods

Standard Protocol Approvals, Registrations, and Patient Consents

The institutional ethical standards committee on human experimentation at IRCCS Ospedale San Raffaele granted approval for experiments involving human subjects (Protocol No. 2015-33). Before participating in the study, all subjects provided written informed consent in accordance with the Declaration of Helsinki.

Study Population

We retrospectively identified 129 consecutive patients with MS and 73 healthy controls (HC) from the Neuroimaging Research Unit database at IRCCS San Raffaele Scientific Institute in Milan, Italy. These individuals had undergone the same MRI protocol between January 2019 and August 2022. Inclusion criteria for patients with MS were age 18 years or older, a diagnosis of MS based on the 2017 revised McDonald criteria, a three-month period free from relapses and steroids before the MRI, absence of significant neurologic (other than MS) or psychiatric conditions that could affect cognitive functioning, and a stable MS treatment for at least 6 months. HC had no neurologic or systemic disorders that could potentially affect the CNS and showed a completely normal neurologic examination.

Neurologic and Neuropsychological Assessment

An experienced neurologist, unaware of MRI results, performed a neurologic examination, rated the Expanded Disability Status Scale (EDSS) score, and defined the MS clinical phenotype (relapsing-remitting or progressive) within 3 days from MRI acquisition.

The Brief Repeatable Battery of Neuropsychological Tests (BRB-N) was administered to all patients with MS on the day of MRI acquisition. Specifically, verbal memory was evaluated with the Selective Recall Test, visual memory with the 10/36 Spatial Recall Test, information processing speed with the SDMT, attention with the PASAT 2" and 3" per digit version, and verbal fluency with the Word List Generation. Z-scores for all BRB-N tests were computed using regression models adjusted for sex, age, and education, based on Italian normative data.²² Then z-scores for distinct cognitive domains were determined by averaging the z-scores of tests within those respective cognitive domains, as previously outlined. Finally, z-scores of cognitive domains were averaged to quantify z-score of global cognitive functions. Test failure was defined as a score 1.5 standard deviations below normative values.²³ Patients with MS with at least one abnormal neuropsychological test in 2 different cognitive domains were classified as cognitively impaired.²³

The Modified form of the Fatigue Impact Scale (MFIS) was used to assess fatigue in 113 of 129 patients with MS (87.6%). The MFIS is a multidimensional scale designed to examine various dimensions of fatigue in daily life. It evaluates the impact on physical, cognitive, and psychosocial domains, characterizing fatigue as a subjective sensation of mismatch between effort exerted and actual performance, in physical, mental, or social contexts.²⁴ Patients with MS who scored 38 or higher on MFIS were defined as fatigued.²⁵

MRI Acquisition

The following brain MRI sequences were acquired using a 3.0 T Philips Ingenia CX scanner (Philips Medical Systems, receiving Coil = dS-Head-32): (a) sagittal three-dimensional

(3D) fluid-attenuated inversion recovery (FLAIR), field of view (FOV) = 256 × 256 mm, voxel size = 1 × 1 × 1 mm, 192 slices, matrix = 256 × 256, repetition time (TR) = 4,800 milliseconds, echo time (TE) = 270 milliseconds, inversion time (TI) = 1,650 milliseconds, echo train length (ETL) = 167, acquisition time = 6.15 minutes; (b) sagittal 3D T1-weighted turbo field echo, FOV = 256 × 256, voxel size = 1 × 1 × 1 mm, 204 slices, matrix = 256 × 256, TR = 7 milliseconds, TE = 3.2 milliseconds, TI = 1,000 milliseconds, flip angle = 8°, acquisition time = 8.53 minutes; (c) 3D T2-weighted scan, FOV = 256 × 256 mm, pixel size = 1 × 1 mm, 192 axial slices with 1-mm slice thickness, TR = 2,500 milliseconds, TE = 330 milliseconds, ETL = 117, acquisition time = 3 minutes; and (d) 3D susceptibility-weighted imaging (SWI), FOV = 230 × 230, pixel size = 0.60 × 0.60 mm, 135 slices, 2-mm thick, matrix = 384 × 382, TR = 39 milliseconds, TEs = 5.5:6:35.5 milliseconds, flip angle = 17°, acquisition time = 6 minutes; magnitude and phase images for every echo were both saved.

For each MRI scan, the slices were oriented parallel to a line connecting the most inferoanterior and inferoposterior margins of the corpus callosum.

Conventional MRI Analysis

A fully automated method, using the 3D FLAIR and 3D T1-weighted as input images, was used to identify brain T2-hyperintense WM lesions.²⁶ The lesion mask, generated by the automated segmentation, was carefully visually checked for each patient, and the volume of T2-hyperintense WM lesions was obtained.

Normalized volumes of the brain, thalamus, caudate, hippocampus, cortex, WM, and ventricles were quantified on 3D T1-weighted images, after lesion refilling, using FSL-SIENAx software and the FSL-FIRST tool, and applying the scaling factor derived from FSL-SIENAx. To calculate the volume of lateral ventricles, the ventricular masks obtained from FSL-SIENAx were used, after manual removal of the third and fourth ventricles.

SWI Processing

Local B0 field change maps were generated from the multi-echo SWIs using the software accessible at github. The initial step involved unwrapping phase images to eliminate discontinuities arising from the restricted range of phase values, employing the best path method.²⁷

Then, a magnitude-weighted least square regression was applied to fit the unwrapped phase images to the echo time. To visualize the paramagnetic rim, we eliminated global spatial changes of the main magnetic field by using regularization enabled sophisticated harmonic artifact reduction for phase data.²⁸

The 3D FLAIR image and the T2-hyperintense WM lesion mask were then both registered onto the SWI space. This registration was achieved using the magnitude of the first echo

of the SWI sequence as the reference image since it contains anatomical information. Rigid transformations were applied to minimize the normalized mutual information as cost function, using FLIRT (FMRIB's Linear Image Registration Tool) which is embedded in the FSL.

Quantification of PRL Number and Volume

For each patient, the number and volume of total T2-hyperintense WM lesions and T2-hyperintense WM lesions with or without the hypointense paramagnetic rim (i.e., PRLs and non-PRLs) were automatically estimated using an in-house implemented method with MATLAB v2012.

First, from the global lesion mask, different intensity values were manually given according to the different type of lesions (1 = non-PRL, 2 = PRL) creating a new label mask.

PRLs were defined as discrete FLAIR hyperintense lesions either completely or partially surrounded by a paramagnetic rim of hypointense signal in unwrapped phase images (Figure 1) by 2 independent raters (P.P. and Y.Y.). In case of disagreement, a third rater (M.A.R.) evaluated the lesions and reached a final decision with the agreement of the other 2 raters.

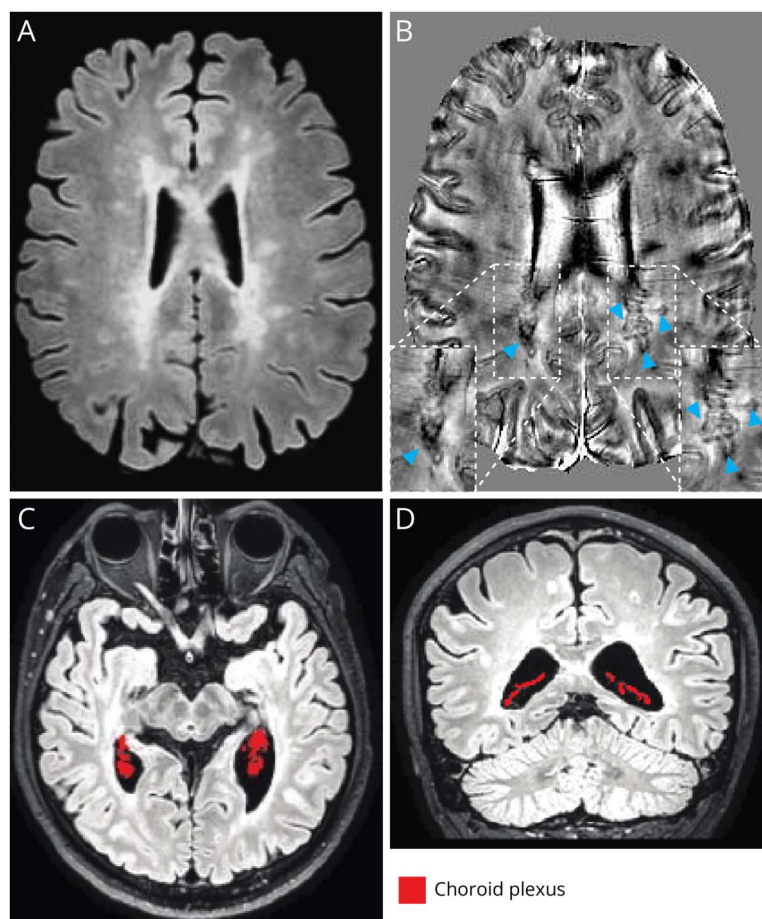
Then, an automatic pipeline estimated the number and the dimension of the 3D connected objects (lesions) found within label masks, separately for each type of lesion (intensity value). The total number of T2-hyperintense WM lesions was obtained from the sum of PRLs and non-PRLs. Volumes were finally obtained by multiplying the dimension for the voxel size.

CP Segmentation and Volume Quantification

CP segmentation was performed using a fully automatic method that was implemented in-house and that started from the brain tissue segmentation derived from the FSL-SIENAX toolbox (Figure 1).²⁹

In particular, the lateral ventricle mask in the standard MNI-152 atlas space underwent an affine registration into the subject space. Then, it was eroded with a filter dimension of 1 mm trying to be conservative as much as possible.³⁰ The coregistered lateral ventricle mask was then used as a template to distinguish peripheral from ventricular CSF on the global CSF segmentation for each subject. WM, GM, and T2-hyperintense lesion tissue masks were subtracted to lateral ventricle mask for each subject to eventually remove also residual boundaries that may share image intensities that are

Figure 1 Examples of Paramagnetic Rim Lesions Identification and Choroid Plexus Segmentation



(A) On 3D axial fluid-attenuated inversion recovery (FLAIR) sequence, multiple T2-hyperintense white matter lesions are visible in a 51-year-old man with relapsing-remitting MS (disease duration = 14 years, Expanded Disability Status Scale [EDSS] score = 4.0). (B) On unwrapped phase image, several paramagnetic rim lesions (light blue arrowheads, also magnified) were found. Example of automatic choroid plexus segmentation (red-coded) on (C) axial and (D) coronal planes of a 3D FLAIR sequence obtained from a 39-year-old woman, with relapsing-remitting MS (disease duration = 9 years, EDSS score = 2.0). See text for further details.

similar to those of the CP on the FLAIR contrast. The resulting “cleaned” ventricle mask was registered into the FLAIR space, and the corresponding image intensities were then extracted. Given that CP are hyperintense on FLAIR, whereas the signal of the CSF is suppressed, we fitted a Gaussian Mixture Model (GMM) with 2 Gaussian distributions to data using the iterative Expectation-Maximization algorithm.³¹ The voxels associated with the Gaussian distribution featuring lower image intensities (i.e., similar to the CSF) were removed. A mean image filtering was applied to the binary mask, which were previously obtained. This aimed to enhance the distinctions between voxels belonging to the CP and spurious boundary voxels. A second GMM, again with 2 Gaussian distributions, was then applied to the previously filtered binary mask. Subsequently, residual clusters of voxels with a dimension less than 3 mm were removed. The obtained mask was the final CP segmentation. The algorithm has been implemented in MATLAB (R2017a, Mathworks). All the generated segmentations of the CP underwent a careful visual inspection, and manual corrections were performed in case of inaccuracies.

Statistical Analysis

Differences of demographic and clinical variables between patients with MS and HC, as well as in patients with MS according to the presence of cognitive impairment or fatigue, were assessed using appropriate statistical tests, including the chi-square, two-sample *t* and Mann-Whitney *U* tests. Between-group comparisons of brain volumetric measures were assessed using age-adjusted and sex-adjusted linear models. Normalized lateral ventricle volume and normalized brain volume were included as additional covariates in the analyses of CP volume, as previously done.¹⁶ T2-hyperintense WM lesion volume was log-transformed. The number and volume of all T2-hyperintense WM lesions, PRLs, and non-PRLs were compared between patients with MS with and without cognitive impairment or fatigue using age-adjusted and sex-adjusted negative binomial and linear regression models, respectively. Differences in the prevalence of at least one PRL as well as in the proportion of PRL number and volume were tested using age-adjusted and sex-adjusted logistic and quasibinomial regression models. To account for the overall number of pairwise comparisons, false discovery rate (FDR) (Benjamini-Hochberg procedure) correction was performed.

Random forest probability models were grown to rank demographic factors (age, sex, and education), clinical variables (EDSS score, disease duration, and clinical phenotype), and MRI measures (lesional and volumetric measures) based on their contribution to the presence of cognitive impairment or fatigue in patients with MS. Specifically, we used the Boruta algorithm, implementing 10,000 trees and 2,000 iterations, to identify a subset of pertinent features.³² The algorithm selects features that outperform randomness by iteratively comparing variables importance metric with those of shadow attributes, which are created by shuffling the original ones. Features with significantly lower importance than shadow attributes, based on binomial tests adjusted for multiple comparisons, are

progressively discarded. The discriminative capability of the new model, trained solely with the selected predictors, was assessed by the out-of-bag area under the curve (OOB-AUC), computed on the left-out observations.

Computations were conducted using SAS release 9.4 (SAS Institute, Cary, NC) and R software (version 4.2.2). Statistical significance was set at *p* values <0.05.

Data Availability

The corresponding author, who had complete access to all the data of the study, assumes responsibility for the integrity of the data and accuracy in the analysis. The anonymized data set used and analyzed for this study can be obtained from the corresponding author on reasonable request.

Results

Demographic, Clinical, and Conventional MRI Variables in Patients With MS Compared With HC

Table 1 summarizes the main demographic, clinical, and MRI features of HC and MS patients.

Compared with HC, patients with MS had significantly higher T2-hyperintense WM lesion number and volume ($p < 0.001$ for both), as well as significantly lower years of education ($p < 0.001$), normalized brain ($p < 0.001$), thalamic ($p < 0.001$), caudate ($p = 0.026$), hippocampal ($p = 0.026$), cortical ($p = 0.040$), WM volumes ($p < 0.001$), and enlarged lateral ventricle volume ($p < 0.001$) (Table 1).

PRLs and CP Volume in MS Patients

Table 1 and Figure 2 present the prevalence, number, and volume of PRLs in patients with MS. Fifty-nine (45.7%) patients with MS had at least one PRL. The median number of PRLs was 0 (interquartile range [IQR] = 0–2), and the median PRL volume was 0.00 mL (0.00–0.65). Among T2-hyperintense WM lesions, the median proportions (IQR) of PRLs and PRL volume were 0.00% (0.00–0.04) and 0.00% (0.00–0.20), respectively.

Compared with HC, patients with MS had significantly higher CP volume (HC: estimated mean [standard error, SE] = 2.18 mL [0.06]; MS patients: estimated mean [SE] = 2.59 [0.05], $p = 0.001$) (Table 1 and Figure 2).

Prevalence of Cognitive Impairment and Relation With PRLs Burden and CP Volume

Thirty-six (27.9%) patients with MS were classified as cognitively impaired. The most frequently affected cognitive domains included verbal memory (81% of cognitively impaired MS patients), attention (61% of cognitively impaired MS patients), and verbal fluency (53% of cognitively impaired MS patients) (Table 2). Performance and prevalence of patients with MS showing impairment at each test of the BRB-N are summarized in Table 2.

Table 1 Main Demographic, Clinical, and MRI Features of HC and MS Patients

Variables	HC (n = 73)	MS (n = 129)	MS vs HC p value
Sex (%): Women/Men	43 (59)/30 (41)	73 (57)/56 (43)	0.749 ^a
Mean age (SD) [y]	41.0 (12.4)	43.3 (11.1)	0.187 ^b
Median disease duration (IQR) [y]	—	9.14 (1.73–19.30)	—
Median EDSS score (IQR)	—	2.0 (1.0–4.0)	—
Clinical phenotype (%): RRMS/PMS	—	94 (73)/35 (27)	—
Ongoing DMT (%) ^h : none/first line/second line	—	12 (9)/73 (57)/44 (34)	—
Median education (IQR) [y]	17 (13–18)	13 (13–17)	<0.001 ^c
Number (%) of cognitively impaired subjects	—	36 (27.9)	—
Number (%) of subjects with fatigue	—	31/113 (27.4)	—
Median number of T2-hyperintense WM lesions (IQR)	0 (0–1)	43 (24–79)	<0.001 ^d
Median T2-hyperintense WM LV (IQR) [mL] ^g	0.00 (0.00–0.21)	2.58 (0.88–6.93)	<0.001 ^e
Number (%) of subjects with ≥1 PRL	0 (0.0%)	59 (45.7)	—
Median PRL number (IQR)	—	0 (0–2)	—
Median proportion of PRLs (IQR) [%]	—	0.00 (0.00–0.04)	—
Median PRL volume (IQR) [mL] ^g	—	0.00 (0.00–0.65)	—
Median proportion of PRL volume (IQR) [%]	—	0.00 (0.00–0.20)	—
Median non-PRL number (IQR)	0 (0–1)	41 (24–72)	<0.001 ^d
Median non-PRL volume (IQR) [mL] ^g	0.00 (0.00–0.21)	2.15 (0.88–5.23)	<0.001 ^e
Estimated mean (SE)			
NBV [mL]	1,554 (5)	1,520 (5)	<0.001 ^e
Normalized thalamic volume [mL]	22.1 (0.1)	20.5 (0.2)	<0.001 ^e
Normalized caudate volume [mL]	9.8 (0.1)	9.5 (0.1)	0.026 ^e
Normalized hippocampal volume [mL]	10.8 (0.1)	10.3 (0.1)	0.002 ^e
Normalized cortical volume [mL]	652 (3)	643 (3)	0.040 ^e
Normalized WM volume [mL]	687 (3)	666 (3)	<0.001 ^e
Normalized CP volume [mL]	2.18 (0.06)	2.59 (0.05)	0.001 ^f
Normalized lateral ventricle volume [mL]	20.4 (1.1)	29.3 (1.3)	<0.001 ^e

Abbreviations: CP = choroid plexus; DMT = disease-modifying therapy; EDSS = expanded disability status scale; HC = healthy controls; IQR = interquartile range; LV = lesion volume; mL = milliliter; NBV = normalized brain volume; PRL = paramagnetic rim lesions; RR = relapsing remitting; P = progressive; SE = standard error; WM = white matter.

^a Chi-square test.

^b Two-sample *t* test.

^c Mann-Whitney *U* Test.

^d Age-adjusted and sex-adjusted negative binomial regression model.

^e Age-adjusted and sex-adjusted linear regression model.

^f Age-adjusted, sex-adjusted, normalized brain, and lateral ventricle volume-adjusted linear regression model.

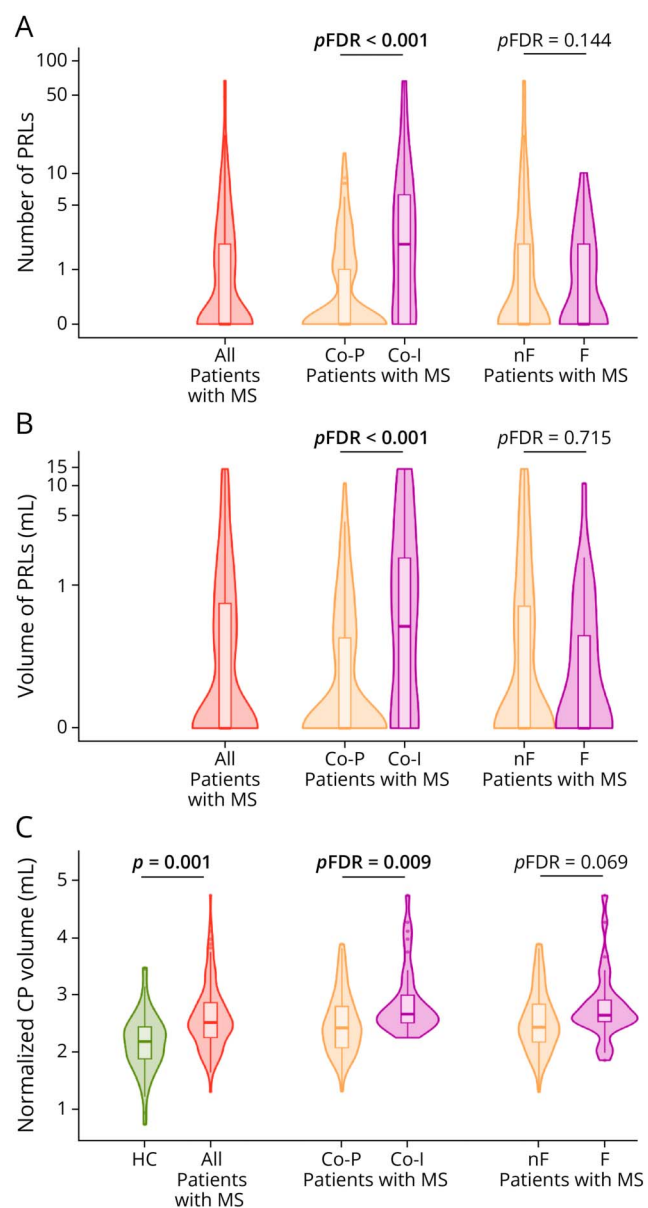
^g Comparison performed on log scale.

^h First line = glatiramer acetate, interferon beta 1a, teriflunomide or dimethyl fumarate; Second line = fingolimod, natalizumab, cladribine, ocrelizumab, rituximab, other immunosuppressants.

Compared with cognitively preserved, patients with cognitively impaired MS were significantly older (pFDR = 0.003), had lower years of education (pFDR = 0.004), higher EDSS score (pFDR = 0.002), were more frequently progressive MS (pFDR = 0.011), and were more frequently untreated

(pFDR = 0.004). Patients with cognitively impaired MS had also higher T2-hyperintense WM lesion number (pFDR = 0.001) and volume (pFDR = 0.003), as well as lower normalized brain (pFDR < 0.001), thalamic (pFDR = 0.005), caudate (pFDR < 0.001), hippocampal (pFDR = 0.005),

Figure 2 Number and Volume of PRLs and CP Volume in Patients With Multiple Sclerosis According to the Presence of Cognitive Impairment and Fatigue



Violin plots show PRL number (A) and volume (B) as well as normalized CP plexus volume distribution in patients with MS according to the presence of cognitive impairment (Co-P and Co-I) or fatigue (nF and F). In (C), normalized CP plexus volume distribution in patients with MS compared with HC is also shown. *p* values of between-group comparisons are also reported (significant comparisons are shown in bold). See text for further details. Co-I = cognitively impaired; Co-P = cognitively preserved; CP = choroid plexus; F = fatigued; mL = milliliter; nF = nonfatigued; *pFDR* = False Discovery Rate *p* value; PRLs value; PRLs = paramagnetic rim lesions.

cortical volumes ($p_{FDR} = 0.001$), and higher lateral ventricle volume ($p_{FDR} = 0.002$).

The proportion of patients showing at least one PRL was significantly higher in cognitively impaired (24/36, 66.7%) compared with patients with cognitively preserved MS (35/93, 37.6%) ($p_{FDR} = 0.006$). Compared with cognitively preserved,

patients with cognitively impaired MS had significantly higher number ($p_{FDR} < 0.001$) and proportion ($p_{FDR} = 0.001$) of PRLs as well as higher PRL volume ($p_{FDR} < 0.001$) and proportion of PRL volume ($p_{FDR} = 0.003$) (Table 3 and Figure 2). Compared with cognitively preserved, patients with cognitively impaired MS had also significantly higher number ($p_{FDR} = 0.003$) and volume ($p_{FDR} = 0.014$) of non-PRLs (Table 3).

Compared with cognitively preserved, patients with cognitively impaired MS had significantly higher CP volume (cognitively preserved MS patients: estimated mean [SE] = 2.51 mL [0.06]; cognitively impaired MS patients: estimated mean [SE] = 2.82 [0.09], $p_{FDR} = 0.009$) (Table 3 and Figure 2).

Prevalence of Fatigue and Relation With PRLs Burden and CP Volume

In total, 31/113 (27.4%) patients with MS were classified as fatigued (Table 3). Compared with nonfatigued, patients with MS with fatigue had significantly higher EDSS score ($p = 0.034$, not surviving FDR correction $p_{FDR} = 0.060$). No significant between-group differences for the other demographic, clinical, and conventional MRI variables were found ($p_{FDR} \geq 0.133$) (Table 3).

The proportion of patients showing at least one PRL, the number and proportion of PRLs, as well as PRL volume and proportion of PRL volume were not significantly different between patients with MS with or without fatigue ($p_{FDR} \geq 0.144$) (Table 3 and Figure 2). Similarly, no significant between-group difference was found for non-PRL number and volume ($p_{FDR} \geq 0.563$).

Compared with nonfatigued MS patients, those with fatigue had significantly higher CP volume (nonfatigued MS patients: estimated mean [SE] = 2.53 mL [0.06]; fatigued MS: estimated mean [SE] = 2.77 [0.10], $p = 0.040$), not surviving FDR correction $p_{FDR} = 0.069$) (Table 3 and Figure 2).

Predictors of Cognitive Impairment and Fatigue in Patients With MS

Table 4 and Figure 3 present the variables selected by Boruta algorithm as relevant predictors of the presence of cognitive impairment and fatigue in patients with MS.

Informative predictors of the presence of cognitive impairment (relative importance) (OOB-AUC = 0.707) were lower NBV (100%), lower normalized caudate volume (89.1%), higher normalized CP volume (80.3%), lower normalized cortical volume (70.3%), higher number (67.3%) and volume of PRLs (66.7%), and higher T2-hyperintense WM volume (64.0%).

Higher normalized CP volume was the only predictor of the presence of fatigue (OOB-AUC = 0.563).

Table 2 Mean z-Scores and Prevalence of Impairment at Neuropsychological Tests and at Each Cognitive Domain Explored by the BRB-N in MS Patients According to Cognitive Status

BRB-N tests	Co-P MS patients (n = 93)		Co-I MS patients (n = 36)		Cognitive domains	Co-P MS patients (n = 93)		Co-I MS patients (n = 36)	
	Z-score ^a	N of impaired ^b (%)	Z-score ^a	N of impaired ^b (%)		Z-score	N of impaired ^c (%)	Z-score	N of impaired ^c (%)
SRT ltr	-0.39 (0.87)	10 (11)	-1.60 (0.84)	19 (53)	Verbal memory	-0.31 (0.87)	15 (16)	-1.64 (0.72)	29 (81)
SRT cltr	-0.33 (0.87)	10 (11)	-1.51 (0.68)	19 (53)					
SRT recall	-0.21 (1.04)	11 (12)	-1.82 (1.06)	22 (61)					
SPART	-0.16 (0.89)	1 (1)	-0.99 (0.86)	10 (28)	Visual memory	0.14 (0.80)	4 (4)	-0.94 (0.82)	16 (44)
SPART recall	-0.12 (0.86)	4 (4)	-0.89 (0.99)	10 (28)					
SDMT	0.17 (1.19)	5 (5)	-1.50 (1.25)	17 (47)	Information processing speed	0.17 (1.19)	5 (5)	-1.50 (1.25)	17 (47)
PASAT 3"	-0.21 (0.95)	9 (10)	-1.58 (1.30)	19 (53)	Attention	-0.23 (0.78)	9 (10)	-1.56 (1.09)	22 (61)
PASAT 2"	-0.33 (0.83)	2 (2)	-1.56 (0.98)	17 (47)					
WLG	-0.19 (0.91)	0 (0)	-1.28 (1.11)	19 (53)	Verbal fluency	-0.01 (0.91)	0 (0)	-1.28 (1.11)	19 (53)
					Global cognition	-0.03 (0.55)	0 (0)	-1.31 (0.60)	36 (100)

Abbreviations: BRB-N = brief repeatable battery of neuropsychological tests; Co-I = cognitively impaired; Co-P = cognitively preserved; cltr = consistent long-term retrieval; ltr = long-term storage; MS = MS; PASAT = paced auditory serial attention test; SDMT = symbol digit modalities test; SPART = spatial recall test; SRT = selective reminding test; WLG = word list generation.

^a Mean (SD) of z-scores according to the normative data of an Italian representative sample.²²

^b Number of patients (frequency) with an abnormal performance, defined as a score 1.5 SD below normative values according to the normative data of an Italian representative sample.²²

^c Number of patients (frequency) with ≥ 1 abnormal neuropsychological tests of BRB-N for each cognitive domain.³⁵

Discussion

In this study, we found that a substantial proportion of patients with MS showed one or more PRLs, and they were also characterized by a significant CP enlargement compared with HC. Higher number and volume of PRLs and higher CP volume were informative predictors of cognitive impairment in addition to atrophy of the whole brain and of strategic and clinically relevant brain GM areas, including the caudate nucleus and the cortex. A higher CP volume was the only variable able to explain the presence of fatigue in our sample.

Fifty-nine of 129 (45.7%) patients with MS showed at least one PRL, which is in line with previous studies where PRL prevalence varied between 6% and 53% in patients with clinically isolated syndrome/relapsing-remitting sclerosis patients and between 7% and 62% in patients with progressive MS.^{9,11,33} The heterogeneous prevalence of PRLs across studies can be due to several factors. Visual evaluation of PRLs may be challenging, and different criteria have been applied for their identification. Furthermore, a recent meta-analysis suggested that demographic and clinical characteristics of patients with MS, including age and disease duration, along with differences in MRI field strengths and sequences used to identify PRLs may contribute to explain heterogeneities regarding the prevalence and number of PRLs among studies.³³

Patients with MS were also characterized by a significant CP enlargement compared with HC, thus supporting the prevailing hypothesis that CP enlargement may be an early phenomenon in MS reflecting CNS chronic inflammation.¹³⁻¹⁷

In our cohort, mainly including patients with relapsing-remitting MS and relatively mild disability, the prevalence of cognitive impairment (27.9%) was consistent with previous studies showing a prevalence ranging between 20-30%, although a higher prevalence (up to 46%) has been reported in other studies.³⁴ Considering the pattern of cognitive deficits, we confirmed that verbal memory, attention, and information processing speed were the most frequently affected domains.^{1,35}

In line with the literature,^{1,4,36} we found that the presence of cognitive impairment was associated with a higher T2-hyperintense WM lesion number and volume, supporting the hypothesis of a 'disconnection syndrome' as one of the most relevant processes contributing to cognitive dysfunction in MS.

The possibility to identify PRLs using SWI allowed us to better characterize the heterogeneous pathologic and microstructural features of T2-hyperintense WM lesions that cannot be directly explored with conventional MRI. Previous studies suggested that the presence of PRLs may be associated with worse cognitive performance in some

Table 3 Main Demographic, Clinical, and MRI Features of MS Patients According to Cognitive Status and the Presence of Fatigue

Variables	Co-P MS patients (n = 93)	Co-I MS patients (n = 36)	Co-I vs Co-P MS patients p value (pFDR)	nF MS patients (n = 82)	F MS patients (n = 31)	F vs nF MS patients p value (pFDR)
Sex (%): Women/Men	52 (56)/41 (44)	21 (58)/15 (42)	0.804 ^a (0.865)	43 (52)/39 (48)	21 (68)/10 (32)	0.143 ^a (0.211)
Mean age (SD) [y]	41.4 (11.0)	48.0 (9.9)	0.001 ^b (0.003)	42.3 (11.0)	45.1 (12.0)	0.257 ^b (0.348)
Median disease duration (IQR) [y]	8.21 (1.18–17.58)	10.90 (4.15–24.50)	0.049 ^c (0.084)	9.07 (1.60–17.95)	5.00 (1.10–17.58)	0.743 ^c (0.821)
Median EDSS score (IQR)	1.5 (1.0–3.0)	3.0 (2.0–6.0)	0.001 ^c (0.002)	1.5 (1.0–3.0)	2.0 (1.5–6.0)	0.034 ^c (0.060)
Clinical phenotype (%): RRMS/PMS	74 (80)/19 (20)	20 (56)/16 (44)	0.006 ^a (0.011)	66 (80)/16 (20)	21 (68)/10 (32)	0.151 ^a (0.219)
Ongoing DMT (%) #: none/first line/second line	4 (4)/60 (65)/29 (31)	8 (22)/13 (36)/15 (42)	0.001 ^d (0.004)	5 (6)/50 (61)/27 (33)	5 (16)/16 (52)/10 (32)	0.235 ^d (0.340)
Median education (IQR) [y]	13 (13–18)	13 (8–15)	0.002 ^c (0.004)	13 (13–17)	13 (8–16)	0.068 ^c (0.113)
Median number of T2-hyperintense WM lesions (IQR)	38 (23–65)	67 (38–102)	<0.001 ^e (0.001)	38 (23–69)	56 (31–82)	0.620 ^e (0.713)
Median T2-hyperintense WM LV (IQR) [mL] ^j	2.01 (0.82–4.29)	6.12 (2.07–13.43)	0.001 ^f (0.003)	2.17 (0.85–6.81)	2.69 (0.83–5.43)	0.892 ^f (0.929)
Number (%) of subjects with ≥1 PRL	35 (37.6)	24 (66.7)	0.003 ^g (0.006)	35 (42.7%)	15 (18.4%)	0.493 ^g (0.592)
Median PRL number (IQR)	0 (0–1)	2 (0–7)	<0.001 ^e (<0.001)	0 (0–2)	0 (0–2)	0.089 ^e (0.144)
Median proportion of PRLs (IQR) [%]	0.00 (0.00–0.03)	0.03 (0.00–0.06)	<0.001 ^h (0.001)	0.00 (0.00–0.05)	0.00 (0.00–0.04)	0.328 ^h (0.417)
Median PRL volume (IQR) [mL] ^j	0.00 (0.00–0.27)	0.37 (0.00–1.90)	<0.001 ^f (<0.001)	0.00 (0.00–0.65)	0.00 (0.00–0.31)	0.638 ^f (0.715)
Median proportion of PRL volume (IQR) [%]	0.00 (0.00–0.12)	0.16 (0.00–0.35)	0.001 ^h (0.003)	0.00 (0.00–0.26)	0.00 (0.00–0.16)	0.182 ^h (0.255)
Median non-PRL number (IQR)	36 (22–62)	65 (37–91)	0.001 ^e (0.003)	36 (23–66)	53 (29–80)	0.456 ^e (0.563)
Median non-PRL volume (IQR) [mL] ^j	1.67 (0.67–3.52)	4.20 (1.81–6.85)	0.008 ^f (0.014)	1.80 (0.85–4.15)	2.40 (0.83–4.32)	0.598 ^f (0.698)
Estimated mean (SE)						
NBV [mL]	1,532 (5)	1,490 (8)	<0.001 ^f (<0.001)	1,525 (5)	1,524 (9)	0.907 ^f (0.929)
Normalized thalamic volume [mL]	20.8 (0.2)	19.7 (0.3)	0.003 ^f (0.005)	20.6 (0.2)	20.9 (0.3)	0.391 ^f (0.490)
Normalized caudate volume [mL]	9.7 (0.1)	8.8 (0.2)	<0.001 ^f (<0.001)	9.6 (0.1)	9.4 (0.2)	0.309 ^f (0.399)
Normalized hippocampal volume [mL]	10.5 (0.1)	9.8 (0.2)	0.003 ^f (0.005)	10.4 (0.1)	10.4 (0.2)	0.947 ^f (0.959)
Normalized cortical volume [mL]	650 (3)	625 (5)	<0.001 ^f (0.001)	646 (3)	646 (3)	0.972 ^f (0.972)
Normalized WM volume [mL]	668 (3)	660 (5)	0.160 ^f (0.227)	667 (3)	666 (6)	0.907 ^f (0.929)
Normalized CP volume [mL]	2.51 (0.06)	2.82 (0.09)	0.004 ⁱ (0.009)	2.53 (0.06)	2.77 (0.10)	0.040 ^f (0.069)
Normalized lateral ventricle volume [mL]	26.6 (1.4)	36.4 (2.4)	0.001 ^f (0.002)	28.0 (1.5)	28.3 (2.4)	0.899 ^f (0.929)

Abbreviations: Co-I = cognitively impaired; Co-P = cognitively preserved; CP = choroid plexus; DMT = disease-modifying therapy; EDSS = expanded disability status scale; F = fatigued; HC = healthy controls; IQR = interquartile range; LV = lesion volume; mL = milliliter; NBV = normalized brain volume; nF = nonfatigued; pFDR = false discovery rate p value; PRL = paramagnetic rim lesions; RR = relapsing remitting; Pr = progressive; SE = standard error; WM = white matter.

^a Chi-square test.

^b Two-sample t test.

^c Mann-Whitney U Test.

^d Fisher exact test.

^e Age-adjusted and sex-adjusted negative binomial regression model.

^f Age-adjusted and sex-adjusted linear regression model.

^g Age-adjusted and sex-adjusted logistic regression model.

^h Age-adjusted and sex-adjusted quasibinomial regression model.

ⁱ Age-adjusted, sex-adjusted, normalized brain, and lateral ventricle volume-adjusted linear regression model.

^j Comparison performed on log scale.

^k First line = glatiramer acetate, interferon beta 1a, teriflunomide or dimethyl fumarate; 2nd line = fingolimod, natalizumab, cladribine, ocrelizumab, rituximab, other immunosuppressants.

Table 4 Random Forest Informative Predictors of Cognitive Impairment and Fatigue in Patients With MS

Outcome	Predictor	Median importance (IQR)	RI	OOB-AUC
Cognitive impairment	NBV	29.8 (27.6–32.1)	100.0	0.707
	Normalized caudate volume	26.5 (24.2–28.8)	89.1	
	Normalized CP volume	23.9 (21.9–26.0)	80.3	
	Normalized cortical volume	20.9 (18.9–23.1)	70.3	
	PRL number	20.0 (18.5–21.6)	67.3	
	PRL volume	19.9 (18.0–22.0)	66.7	
	T2-hyperintense WM LV	19.1 (17.5–20.6)	64.0	
Fatigue	Normalized CP volume	19 (14.7–24.1)	100	0.563

Abbreviations: CP = choroid plexus; IQR = interquartile range; LV = lesion volume; NBV = normalized brain volume; OOB-AUC = out-of-bag area under the curve; PRL = paramagnetic rim lesions; RI = relative importance; WM = white matter. Variables selected by Boruta algorithm as relevant predictors of the presence of cognitive impairment and fatigue in patients with MS are listed. Median importance of each predictor, achieved across iterations, the RI, and the performance of a final random forest model including only selected variables are also reported.

neuropsychological tests that mainly explore attention and information processing speed.^{10,19,20} The availability of a validated and comprehensive neuropsychological assessment and the quantification of PRL number and volume in a large cohort of patients allowed us to better explore the association between PRL burden and cognitive impairment. We found that the proportion of patients showing at least one PRL, as well as the total number and volume of PRLs, were significantly higher in patients with MS with cognitive impairment compared with those without.

Our results suggest that a higher burden of PRLs may typify MS patients with worse cognitive performance, thus further supporting the key role of chronic inflammation within the CNS as a driver of a more severe disease course. Although we did not directly evaluate microstructural tissue properties of PRLs, previous studies have shown that PRLs are characterized by more severe microstructural tissue abnormalities, in lower T1-hypointensity, lower myelin water fraction, lower neurite density index, and higher mean diffusivity.^{9,37,38} Such a more severe PRL microstructural damage may contribute to explain, at least partially, the results from previous studies showing that the severity of intrinsic WM lesion damage contributes to cognitive impairment by disrupting WM tracts connecting cognitively relevant GM regions.^{4,5}

We also found that both MS patients with and without cognitive impairment showed a significant CP enlargement compared with HC. Interestingly, in the direct comparison, compared with cognitively preserved, patients with cognitively impaired MS showed a significantly higher CP volume. Our results are in line with a recent study showing that CP volume was significantly higher in cognitively impaired compared with patients with cognitively preserved MS according to Montreal Cognitive Assessment scores and that higher CP volume was associated with worse SDMT performance.²¹

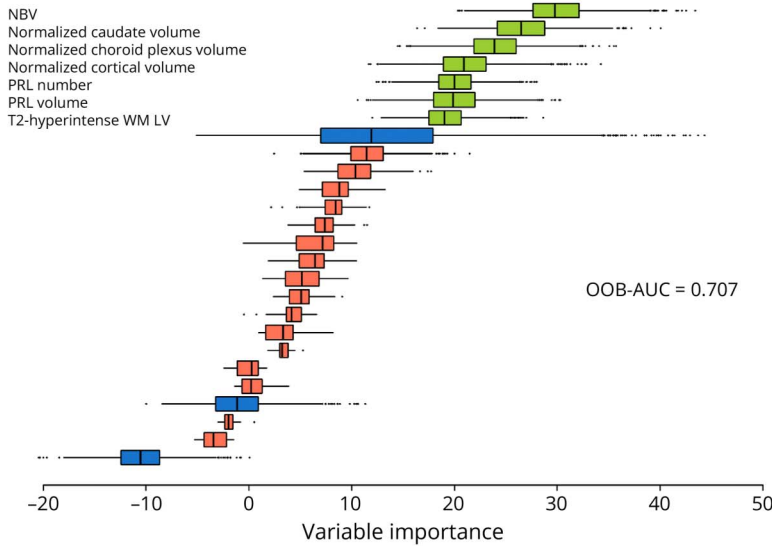
The CP is a relevant interface between the peripheral immune system and the CNS, it represents a gateway for lymphocyte entry from peripheral blood into the CNS, and it is involved in CSF monitoring and antigen presentation.^{39,40} In MS, immune cell aggregates in the CP stroma and vessels, with higher amount of T lymphocytes, macrophages, dendritic cells, and granulocytes and increased expression of vascular adhesion molecules, have been described.^{39,40} Changes in the structure and function of capillaries and ependymal cells including increased permeability of capillaries, thickening of the basement membrane, and loss of cilia in ependymal cells have been also reported.^{39,41} Finally, CP environment may also become hypoxic in patients with MS, determining a dysregulation of Hypoxia-Inducible Factor-1 pathway and then altering secretory and neuroprotective properties of the CP.⁴² Taking all these findings into account, it is likely that, in MS, CP enlargement may reflect structural and functional abnormalities of this structure associated with a chronic proinflammatory state, with an increased immune cell entry and the release of proinflammatory cytokines. These pathologic processes may not only promote demyelination and neuro-axonal loss but also impaired synaptic functioning that play a substantial role not only in disease progression but also in cognitive impairment.

Beside focal WM lesion burden, number, and volume of PRLs and CP enlargement, our study confirmed the relevance of atrophy of the whole brain and of critical GM regions for cognitive impairment, including the thalamus, caudate nucleus, and the cortex.⁴³⁻⁴⁵

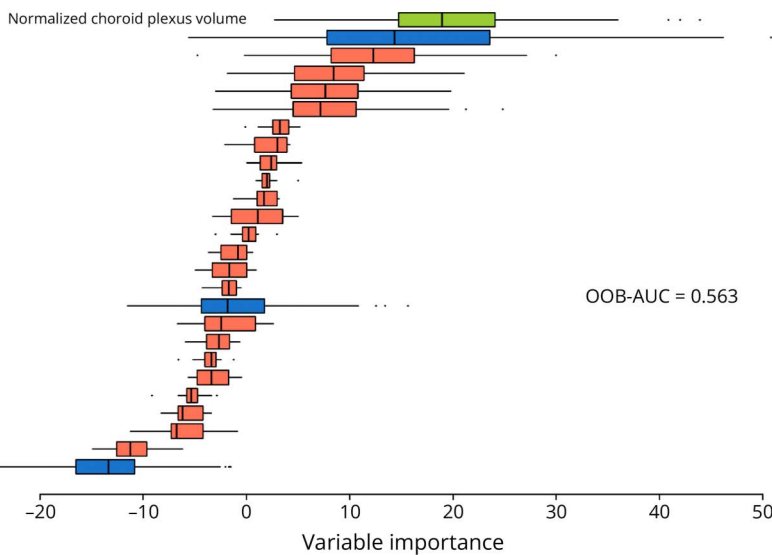
The relevance of combining PRL and CP assessment together with global focal WM lesions and brain volumetric MRI measures is supported by the high accuracy obtained to explain the presence of cognitive impairment by the random forest analysis (OOB-AUC = 0.707). Interestingly, although

Figure 3 Random Forest Informative Predictors of Cognitive Impairment and Fatigue in Patients With Multiple Sclerosis

A. Predictors of cognitive impairment



B. Predictors of fatigue



Distribution of variable importance, achieved across iterations of Boruta algorithm, of demographic, clinical, and MRI features to explain (A) cognitive impairment and (B) fatigue. Boruta compares the importance of the original variables with the highest feature importance of the shadow features, obtained using feature-permuted copies. Poorly performing variables are progressively discarded. Selected features are shown in green, discarded features in red. Maximum, mean, and minimum importance achieved by shadows attributes are shown in blue. LV = lesion volume; NBV = normalized brain volume; OOB-AUC = out-of-bag area under the curve; PRL = paramagnetic rim lesion; WM = white matter.

the number and volume of both PRLs and non-PRLs were found to be significantly associated with cognitive impairment, the results of the random forest analysis suggested that such association is more specific for PRLs in a multivariate setting. Although further studies are necessary to confirm our findings, it is tempting to speculate that chronic inflammation may contribute to cognitive impairment even before and independently from structural brain damage accumulation.

In our cohort, 31/113 (27.4%) patients with MS were classified as fatigued, a prevalence that is lower compared with previous studies.² The predominance of patients with relapsing-remitting MS and relatively low disability scores may contribute to explain this finding. A progressive clinical phenotype and a more severe disability may influence fatigue

levels and may promote limitations in several functional systems, contributing to worsening of perceived fatigue.²⁵ Moreover, previous studies reported very heterogeneous and variable results, with up to 81% of patients with MS having fatigue, possibly due to variations in disease severity, clinical phenotypes, and the methods used for identifying fatigue.²

Interestingly, CP volume was the only significant MRI measure being significantly different in patients with MS according to the presence of fatigue, with a significantly higher CP volume in fatigued compared with nonfatigued MS patients. Although this result did not survive correction for multiple comparison, the relevance of CP enlargement in explaining the presence of fatigue has been further supported by the

random forest analysis, where higher CP volume represented the only informative predictor of the presence of fatigue (OOB-AUC = 0.563).

Different pathophysiologic mechanisms have been proposed to explain fatigue in MS, including immunologic processes occurring within or outside the CNS,^{46,47} together with structural and functional brain MRI abnormalities of specific CNS regions.^{2,6,7}

In line with the potential role of the immune system,^{46,47} CP enlargement may underlie structural and functional abnormalities of this structure that reflect a chronic inflammatory state, with abnormal immune cell migration, localization, and activation within the CNS. These processes may create a chronic inflammatory state in the CNS, with higher levels of proinflammatory cytokines and chemokines and lower levels of anti-inflammatory cytokines, such as interleukin 10. This condition may trigger both central and peripheral pathologic processes, including a reduced synthesis of monoaminergic neurotransmitters such as dopamine, norepinephrine, and serotonin that are involved in motivation, arousal and mood, and impaired synaptic functions and brain network efficiency.⁴⁸⁻⁵¹ All of these mechanisms may lead to abnormal network function, with loss of activity but also with abnormal recruitment of brain regions, either in additional CNS areas or of unusually high levels of activation.^{6,7} Both CP enlargement and fatigue can be found early in the disease course, also independently from clinical disability and disease duration. Accordingly, it is tempting to speculate that CP enlargement may underline chronic inflammatory processes that are likely to contribute to fatigue from the earliest phases of the disease.

Our study has some limitations. Our analyses included a cohort of patients with MS with the main clinical phenotypes. However, the contribution of the different pathologic substrates may be different through MS disease course. Furthermore, the cross-sectional design of the study did not allow to explore the longitudinal interplay between PRLs, CP enlargement, and clinical manifestations. Finally, T1-hypointense lesion volume may be another MRI marker associated with worse cognitive performance. However, we did not acquire a T1-weighted spin-echo sequence that is typically used to detect black holes, but a 3D T1-weighted turbo field echo. Owing to its slight T2* weight in addition to the main T1-weighted contrast, the T1-hypointense lesion volume on this sequence is very similar to that visible on T2-weighted sequences. PRLs are characterized by more severe microstructural damage, also in longer T1 relaxation times compared with non-PRLs.^{52,53} Accordingly, since PRLs are informative predictors of cognitive impairment more than non-PRLs, the presence of lesions that are chronically active but also with more severe microstructural damage may contribute to explain cognitive impairment in patients with MS.

In conclusion, our study showed that PRLs and CP enlargement may represent 2 putative markers of chronic inflammation

contributing to explain cognitive impairment and fatigue in patients with MS. These MRI markers may represent novel and clinically relevant therapeutic targets for future therapies aimed at reducing the detrimental effects of MS not only on clinical disability but also cognitive impairment and fatigue.

Study Funding

The authors report no targeted funding.

Disclosure

The authors declare that they have no competing interests in relation to this work. Potential conflicts of interest outside the submitted work are as follows: P. Preziosa received speaker honoraria from Roche, Biogen, Novartis, Merck Serono, Bristol-Myers Squibb, Genzyme, Horizon and Sanofi, he has received research support from Italian Ministry of Health and Fondazione Italiana Sclerosi Multipla; E. Pagni has nothing to disclose; A. Meani has nothing to disclose; L. Storelli has nothing to disclose; M. Margoni reports grants and personal fees from Sanofi Genzyme, Merck Serono, Novartis and Almiral; Y. Yudin has nothing to disclose; N. Tedone has nothing to disclose; D. Biondi has nothing to disclose; M. Rubin has nothing to disclose; M.A. Rocca received consulting fees from Biogen, Bristol-Myers Squibb, Eli Lilly, Janssen, Roche, and speaker honoraria from AstraZaneca, Biogen, Bristol-Myers Squibb, Bromatech, Celgene, Genzyme, Horizon Therapeutics Italy, Merck Serono SpA, Novartis, Roche, Sanofi and Teva, she receives research support from the MS Society of Canada, the Italian Ministry of Health, the Italian Ministry of University and Research, and Fondazione Italiana Sclerosi Multipla, she is Associate Editor for Multiple Sclerosis and Related Disorders; M. Filippi is Editor-in-Chief of the Journal of Neurology, Associate Editor of Human Brain Mapping, Neurological Sciences, and Radiology, received compensation for consulting services from Alexion, Almirall, Biogen, Merck, Novartis, Roche, Sanofi, speaking activities from Bayer, Biogen, Celgene, Chiesi Italia SpA, Eli Lilly, Genzyme, Janssen, Merck Serono, Neopharmed Gentili, Novartis, Novo Nordisk, Roche, Sanofi, Takeda, and TEVA, participation in Advisory Boards for Alexion, Biogen, Bristol-Myers Squibb, Merck, Novartis, Roche, Sanofi, Sanofi-Aventis, Sanofi Genzyme, Takeda, scientific direction of educational events for Biogen, Merck, Roche, Celgene, Bristol-Myers Squibb, Lilly, Novartis, Sanofi Genzyme, he receives research support from Biogen Idec, Merck Serono, Novartis, Roche, the Italian Ministry of Health, the Italian Ministry of University and Research, and Fondazione Italiana Sclerosi Multipla. Go to [Neurology.org/NN](https://www.neurology.org/NN) for full disclosures.

Publication History

Received by *Neurology: Neuroimmunology & Neuroinflammation* August 7, 2023. Accepted in final form December 18, 2023. Submitted and externally peer reviewed. The handling editor was Deputy Editor Scott S. Zamvil, MD, PhD, FAAN.

Appendix Authors

Name	Location	Contribution
Paolo Preziosa, MD, PhD	Neuroimaging Research Unit, Division of Neuroscience; Neurology Unit, IRCCS San Raffaele Scientific Institute; Vita-Salute San Raffaele University, Milan, Italy	Drafting/revision of the manuscript for content, including medical writing for content; study concept or design; analysis or interpretation of data
Elisabetta Pagani, MSc	Neuroimaging Research Unit, Division of Neuroscience, IRCCS San Raffaele Scientific Institute, Milan, Italy	Drafting/revision of the manuscript for content, including medical writing for content; analysis or interpretation of data
Alessandro Meani, MSc	Neuroimaging Research Unit, Division of Neuroscience, IRCCS San Raffaele Scientific Institute, Milan, Italy	Drafting/revision of the manuscript for content, including medical writing for content; analysis or interpretation of data
Loredana Storelli, PhD	Neuroimaging Research Unit, Division of Neuroscience, IRCCS San Raffaele Scientific Institute, Milan, Italy	Drafting/revision of the manuscript for content, including medical writing for content; analysis or interpretation of data
Monica Margoni, MD, PhD	Neuroimaging Research Unit, Division of Neuroscience; Neurology Unit; Neurorehabilitation Unit, IRCCS San Raffaele Scientific Institute, Milan, Italy	Drafting/revision of the manuscript for content, including medical writing for content; analysis or interpretation of data
Yury Yudin, MD	Neuroimaging Research Unit, Division of Neuroscience, IRCCS San Raffaele Scientific Institute, Milan, Italy	Drafting/revision of the manuscript for content, including medical writing for content; analysis or interpretation of data
Nicolò Tedone, MSc	Neuroimaging Research Unit, Division of Neuroscience, IRCCS San Raffaele Scientific Institute, Milan, Italy	Drafting/revision of the manuscript for content, including medical writing for content; analysis or interpretation of data
Diana Biondi, MSc	Neuroimaging Research Unit, Division of Neuroscience, IRCCS San Raffaele Scientific Institute, Milan, Italy	Drafting/revision of the manuscript for content, including medical writing for content; analysis or interpretation of data
Martina Rubin, MD	Neuroimaging Research Unit, Division of Neuroscience; Neurology Unit, IRCCS San Raffaele Scientific Institute; Vita-Salute San Raffaele University, Milan, Italy	Drafting/revision of the manuscript for content, including medical writing for content; analysis or interpretation of data
Maria A. Rocca, MD	Neuroimaging Research Unit, Division of Neuroscience; Neurology Unit, IRCCS San Raffaele Scientific Institute; Vita-Salute San Raffaele University, Milan, Italy	Drafting/revision of the manuscript for content, including medical writing for content; study concept or design; analysis or interpretation of data
Massimo Filippi, MD	Neuroimaging Research Unit, Division of Neuroscience; Neurology Unit; Vita-Salute San Raffaele University; Neurorehabilitation Unit; Neurophysiology Service, IRCCS San Raffaele Scientific Institute, Milan, Italy	Drafting/revision of the manuscript for content, including medical writing for content; study concept or design; analysis or interpretation of data

References

- Rocca MA, Amato MP, De Stefano N, et al. Clinical and imaging assessment of cognitive dysfunction in multiple sclerosis. *Lancet Neurol.* 2015;14(3):302-317. doi:10.1016/S1474-4422(14)70250-9
- Marchesi O, Vizzino C, Filippi M, Rocca MA. Current perspectives on the diagnosis and management of fatigue in multiple sclerosis. *Expert Rev Neurother.* 2022;22(8):681-693. doi:10.1080/14737175.2022.2106854
- Eijlers AJC, Meijer KA, van Geest Q, Geurts JGG, Schoonheim MM. Determinants of cognitive impairment in patients with multiple sclerosis with and without atrophy. *Radiology.* 2018;288(2):544-551. doi:10.1148/radiol.2018172808
- Mesaros S, Rocca MA, Kacar K, et al. Diffusion tensor MRI tractography and cognitive impairment in multiple sclerosis. *Neurology.* 2012;78(13):969-975. doi:10.1212/WNL.0b013e31824d5859
- Preziosa P, Pagani E, Meani A, et al. NODDI, diffusion tensor microstructural abnormalities and atrophy of brain white matter and gray matter contribute to cognitive impairment in multiple sclerosis. *J Neurol.* 2023;270(2):810-823. doi:10.1007/s00415-022-11415-1
- Arm J, Ribbons K, Lechner-Scott J, Ramadan S. Evaluation of MS related central fatigue using MR neuroimaging methods: scoping review. *J Neurol Sci.* 2019;400:52-71. doi:10.1016/j.jns.2019.03.007
- Bertoli M, Tecchio F. Fatigue in multiple sclerosis: does the functional or structural damage prevail? *Mult Scler.* 2020;26(14):1809-1815. doi:10.1177/1352458520912175
- Matthews PM. Chronic inflammation in multiple sclerosis—seeing what was always there. *Nat Rev Neurol.* 2019;15(10):582-593. doi:10.1038/s41582-019-0240-y
- Dal-Bianco A, Grabner G, Kronnerwetter C, et al. Long-term evolution of multiple sclerosis iron rim lesions in 7 T MRI. *Brain.* 2021;144(3):833-847. doi:10.1093/brain/awaa436
- Absinta M, Sati P, Masuzzo F, et al. Association of chronic active multiple sclerosis lesions with disability in vivo. *JAMA Neurol.* 2019;76(12):1474-1483. doi:10.1001/jamaneurol.2019.2399
- Maggi P, Kuhle J, Schadelin S, et al. Chronic white matter inflammation and serum neurofilament levels in multiple sclerosis. *Neurology.* 2021;97(6):e543-e553. doi:10.1212/WNL.00000000000012326
- Gherzi-Egea JF, Strazielle N, Catala M, Silva-Vargas V, Doetsch F, Engelhardt B. Molecular anatomy and functions of the choroidal blood-cerebrospinal fluid barrier in health and disease. *Acta Neuropathol.* 2018;135(3):337-361. doi:10.1007/s00401-018-1807-1
- Bergsland N, Dwyer MG, Jakimovski D, et al. Association of choroid plexus inflammation on MRI with clinical disability progression over 5 years in patients with multiple sclerosis. *Neurology.* 2023;100(9):e911-e920. doi:10.1212/WNL.00000000000021608
- Fleischer V, Gonzalez-Escamilla G, Ciolac D, et al. Translational value of choroid plexus imaging for tracking neuroinflammation in mice and humans. *Proc Natl Acad Sci U S A.* 2021;118(36):e2025000118. doi:10.1073/pnas.2025000118
- Ricigliano VAG, Morena E, Colombi A, et al. Choroid plexus enlargement in inflammatory multiple sclerosis: 3.0-T MRI and translocator protein PET evaluation. *Radiology.* 2021;301(1):166-177. doi:10.1148/radiol.2021204426
- Margoni M, Gueye M, Meani A, et al. Choroid plexus enlargement in paediatric multiple sclerosis: clinical relevance and effect of sex. *J Neurol Neurosurg Psychiatry.* 2023;94(3):181-188. doi:10.1136/jnnp-2022-330343
- Ricigliano VAG, Louapre C, Poirion E, et al. Imaging characteristics of choroid plexuses in presymptomatic multiple sclerosis: a retrospective study. *Neurol Neuroimmunol Neuroinflamm.* 2022;9(6):e200026. doi:10.1212/NXI.00000000000002026
- Mahad DH, Trapp BD, Lassmann H. Pathological mechanisms in progressive multiple sclerosis. *Lancet Neurol.* 2015;14(2):183-193. doi:10.1016/S1474-4422(14)70256-X
- Marcellè M, Hurtado Rua S, Tyshkov C, et al. Disease correlates of rim lesions on quantitative susceptibility mapping in multiple sclerosis. *Sci Rep.* 2022;12(1):4411. doi:10.1038/s41598-022-08477-6
- Hemond CC, Baek J, Ionete C, Reich DS. Paramagnetic rim lesions are associated with pathogenic CSF profiles and worse clinical status in multiple sclerosis: a retrospective cross-sectional study. *Mult Scler.* 2022;28(13):2046-2056. doi:10.1177/13524585221102921
- Wang X, Zhu Q, Yan Z, et al. Enlarged choroid plexus related to iron rim lesions and deep gray matter atrophy in relapsing-remitting multiple sclerosis. *Mult Scler Relat Disord.* 2023;75:104740. doi:10.1016/j.msard.2023.104740
- Amato MP, Portaccio E, Goretti B, et al. The Rao's Brief Repeatable Battery and Stroop Test: normative values with age, education and gender corrections in an Italian population. *Mult Scler.* 2006;12(6):787-793. doi:10.1177/1352458506070933
- Amato M, Morra V, Falautano M, et al. Cognitive assessment in multiple sclerosis—an Italian consensus. *Neurol Sci.* 2018;39(8):1317-1324. doi:10.1007/s10072-018-3427-x
- Fisk JD, Ritvo PG, Ross L, Haase DA, Marrie TJ, Schlech WF. Measuring the functional impact of fatigue: initial validation of the fatigue impact scale. *Clin Infect Dis.* 1994;18(suppl 1):S79-S83. doi:10.1093/clinids/18.supplement_1.s79
- Marchesi O, Vizzino C, Meani A, et al. Fatigue in multiple sclerosis patients with different clinical phenotypes: a clinical and magnetic resonance imaging study. *Eur J Neurol.* 2020;27(12):2549-2560. doi:10.1111/ene.14471
- Valverde S, Cabezas M, Roura E, et al. Improving automated multiple sclerosis lesion segmentation with a cascaded 3D convolutional neural network approach. *Neuroimage.* 2017;155:159-168. doi:10.1016/j.neuroimage.2017.04.034
- Abdul-Rahman HS, Gdeisat MA, Burton DR, Lator MJ, Lilley F, Moore CJ. Fast and robust three-dimensional best path phase unwrapping algorithm. *Appl Opt.* 2007;46(26):6623-6635. doi:10.1364/ao.46.006623

28. Sun H, Wilman AH. Background field removal using spherical mean value filtering and Tikhonov regularization. *Magn Reson Med*. 2014;71(3):1151-1157. doi:10.1002/mrm.24765
29. Storelli L, Pagani E, Rubin M, Margoni M, Filippi M, Rocca MA. A fully automatic method to segment choroid plexuses in multiple sclerosis using conventional MRI sequences. *J Magn Reson Imaging*. 2023. doi:10.1002/jmri.28937
30. Evans AC, Collins DL, Millst SR, Brown ED, Kelly RL, Peters TM. 3D statistical neuroanatomical models from 305 MRI volumes. In: IEEE, ed. *IEEE Nuclear Science Symposium and Medical Imaging Conference, San Francisco, CA*; 1993:1813-1817.
31. Balafar MA. Gaussian mixture model based segmentation methods for brain MRI images. *Artif Intelligence Rev*. 2012;41(3):429-439. doi:10.1007/s10462-012-9317-3
32. Kursa MB, Rudnicki WR. Feature selection with the Boruta package. *J Stat Softw*. 2010;36(11):1-13. doi:10.18637/jss.v036.i11
33. Ng Kee Kwong KC, Mollison D, Meijboom R, et al. The prevalence of paramagnetic rim lesions in multiple sclerosis: a systematic review and meta-analysis. *PLoS One*. 2021;16(9):e0256845. doi:10.1371/journal.pone.0256845
34. Achiron A, Chapman J, Magalashvili D, et al. Modeling of cognitive impairment by disease duration in multiple sclerosis: a cross-sectional study. *PLoS One*. 2013;8:e71058. doi:10.1371/journal.pone.0071058
35. Ruano L, Portaccio E, Goretti B, et al. Age and disability drive cognitive impairment in multiple sclerosis across disease subtypes. *Mult Scler*. 2017;23(9):1258-1267. doi:10.1177/1352458516674367
36. Rossi F, Giorgio A, Battaglini M, et al. Relevance of brain lesion location to cognition in relapsing multiple sclerosis. *PLoS One*. 2012;7(11):e44826. doi:10.1371/journal.pone.0044826
37. Rahmzadeh R, Lu PJ, Barakovic M, et al. Myelin and axon pathology in multiple sclerosis assessed by myelin water and multi-shell diffusion imaging. *Brain*. 2021;144(6):1684-1696. doi:10.1093/brain/awab088
38. Weber CE, Wittayer M, Kraemer M, et al. Long-term dynamics of multiple sclerosis iron rim lesions. *Mult Scler Relat Disord*. 2022;57:103340. doi:10.1016/j.msard.2021.103340
39. Rodriguez-Lorenzo S, Konings J, van der Pol S, et al. Inflammation of the choroid plexus in progressive multiple sclerosis: accumulation of granulocytes and T cells. *Acta Neuropathol Commun*. 2020;8(1):9. doi:10.1186/s40478-020-0885-1
40. Vercellino M, Votta B, Condello C, et al. Involvement of the choroid plexus in multiple sclerosis autoimmune inflammation: a neuropathological study. *J Neuroimmunol*. 2008;199(1-2):133-141. doi:10.1016/j.jneuroim.2008.04.035
41. Jimenez AJ, Dominguez-Pinos MD, Guerra MM, Fernandez-Llebrez P, Perez-Figares JM. Structure and function of the ependymal barrier and diseases associated with ependyma disruption. *Tissue Barriers*. 2014;2:e28426. doi:10.4161/tisb.28426
42. Rodriguez-Lorenzo S, Ferreira Francisco DM, Vos R, et al. Altered secretory and neuroprotective function of the choroid plexus in progressive multiple sclerosis. *Acta Neuropathol Commun*. 2020;8(1):35. doi:10.1186/s40478-020-00903-y
43. Schoonheim MM, Hulst HE, Brandt RB, et al. Thalamus structure and function determine severity of cognitive impairment in multiple sclerosis. *Neurology* 2015;84(8):776-783. doi:10.1212/WNL.0000000000001285
44. Eijlers AJC, Dekker I, Steenwijk MD, et al. Cortical atrophy accelerates as cognitive decline worsens in multiple sclerosis. *Neurology*. 2019;93(14):e1348-e1359. doi:10.1212/WNL.00000000000008198
45. Sicotte NL, Kern KC, Giesser BS, et al. Regional hippocampal atrophy in multiple sclerosis. *Brain*. 2008;131(Pt 4):1134-1141. doi:10.1093/brain/awn030
46. Gold SM, Kruger S, Ziegler KJ, et al. Endocrine and immune substrates of depressive symptoms and fatigue in multiple sclerosis patients with comorbid major depression. *J Neurol Neurosurg Psychiatry*. 2011;82(7):814-818. doi:10.1136/jnnp.2010.230029
47. Heesen C, Nawrath L, Reich C, Bauer N, Schulz KH, Gold SM. Fatigue in multiple sclerosis: an example of cytokine mediated sickness behaviour?. *J Neurol Neurosurg Psychiatry*. 2006;77(1):34-39. doi:10.1136/jnnp.2005.065805
48. Dantzer R. Neuroimmune interactions: from the brain to the immune system and vice versa. *Physiol Rev*. 2018;98(1):477-504. doi:10.1152/physrev.00039.2016
49. Dantzer R, Heijnen CJ, Kavelaars A, Laye S, Capuron L. The neuroimmune basis of fatigue. *Trends Neurosci*. 2014;37(1):39-46. doi:10.1016/j.tins.2013.10.003
50. Manjaly ZM, Harrison NA, Critchley HD, et al. Pathophysiological and cognitive mechanisms of fatigue in multiple sclerosis. *J Neurol Neurosurg Psychiatry*. 2019;90(6):642-651. doi:10.1136/jnnp-2018-320050
51. Gilio L, Buttari F, Pavone L, et al. Fatigue in multiple sclerosis is associated with reduced expression of interleukin-10 and worse prospective disease activity. *Biomedicines* 2022;10(9):2058. doi:10.3390/biomedicines10092058
52. Absinta M, Sati P, Schindler M, et al. Persistent 7-tesla phase rim predicts poor outcome in new multiple sclerosis patient lesions. *J Clin Invest*. 2016;126(7):2597-2609. doi:10.1172/JCI86198
53. Krajnc N, Schmidbauer V, Leinkauf J, et al. Paramagnetic rim lesions lead to pronounced diffuse periplaque white matter damage in multiple sclerosis. *Mult Scler*. 2023;29(11-12):1406-1417. doi:10.1177/13524585231197954